

Simulation of Flow in PWR Reactor Pressure Vessel Downcomer

Aljaž Kekec, Jure Marn
Faculty of Mechanical Engineering
University of Maribor,
Smetanova ulica 17
SI-2000 Maribor, Slovenia

aljz.kekec@gmail.com, jure.marn@um.si

Ivo Kljenak

Jožef Stefan Institute
Reactor Engineering Division
Jamova cesta 39
SI-1000 Ljubljana, Slovenia
ivo.kljenak@ijs.si

University of Ljubljana
Faculty of Mathematics and Physics
Jadranska ulica 19
SI-1000 Ljubljana, Slovenia
ivo.kljenak@fmf.uni-lj.si

ABSTRACT

The flow in the downcomer of the Reactor Pressure Vessel of a Pressurized Water Reactor was simulated on a local instantaneous scale, using a Computational Fluid Dynamics code. The flow at both normal operation and accident conditions was simulated. In addition, a simulation with different orientation of the cold legs was performed, to illustrate how such simulations may help in the further development of nuclear systems.

1 INTRODUCTION

In a Pressurized Water Reactor (PWR), coolant enters into the downcomer of the Reactor Pressure Vessel (RPV) through two, three or four cold legs, with inlets evenly spaced over the circumference. The mixing of the flow in the downcomer determines the flow conditions (velocity and temperature fields) in the RPV lower plenum and further on in the reactor core. Unfortunately, as the installation of measuring devices in the downcomer would be impractical and costly, and would also unnecessarily disturb the flow, the actual pattern of the flow in the downcomer is not well known. Accurate knowledge of the flow pattern would offer additional insights into the flow phenomena in the RPV.

With the advent of Computational Fluid Dynamics (CFD), the flow in the downcomer may be simulated on the local instantaneous scale, providing a detailed picture of the flow. Although simulations probably do not replicate the flow exactly, the results may still be considered as a reasonable approximation of the actual flow.

Many such simulations have been presented in the literature, which shows the relevance and importance of this topic. The simulations were related either to mixing [1,2], to the pressurized thermal shock following injection of cold water during mitigation of an accident [3,4], or to a possible boron dilution event [5].

In the present work, the flow in the downcomer of a two-loop PWR RPV was simulated on the local instantaneous scale, using the CFD code ANSYS CFX, both at normal operating and at break flow conditions. The flow was assumed to be isothermal, so the issue of pressurized thermal shock was not considered. The simulations provide insights into the velocity field in

the downcomer. Furthermore, a simulation with obliquely (instead of perpendicularly) mounted cold legs was performed to illustrate the applicability of such simulations for further development of nuclear systems, as well, in this specific case, to evaluate whether such a modified design would be more favourable for flow mixing.

2 MODELLING

2.1 Physical model

As the flow was assumed isothermal, only the continuity and momentum equations for an incompressible fluid were solved. As the flow in the downcomer is allegedly turbulent, turbulence was modelled with the k - ε model. Default flow options were mostly used.

2.2 Numerical mesh

A simplified model of a PWR downcomer, suitable for CFD simulations, was defined (Figure 1). After that, a numerical mesh for the CFD code CFX was developed. Figure 2 shows part of the developed mesh. The outlet of the downcomer was defined as an opening boundary condition due to a recirculation problem that occurred during first simulations.

An analysis of numerical accuracy with different mesh refinements was performed. Since fairly similar gradients in the whole downcomer were expected and no specific region of the downcomer is studied in detail, the mesh was uniformly dense throughout the whole computation domain.

Mesh settings were set to default ANSYS CFX settings for CFD. The only parameter that was changed was the element size. Four different sizes were used: 0.1 m, 0.05 m, 0.035 m and 0.032 m. These element sizes resulted in the following number of nodes: 28083, 161145, 400873 and 502957, respectively. The analyses showed, that the simulations with the smallest mesh element converged, so the mesh was considered as adequate.

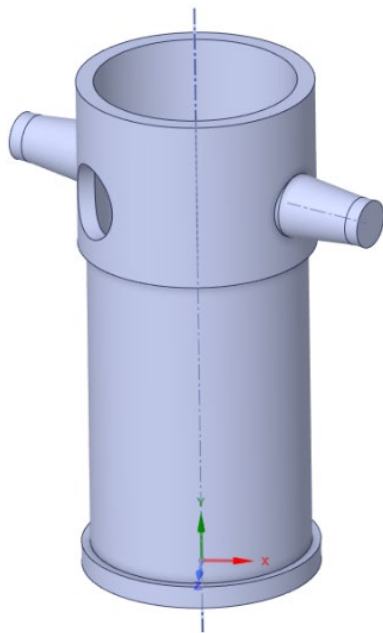


Figure 1. Schematic view of downcomer and cold leg inlets.

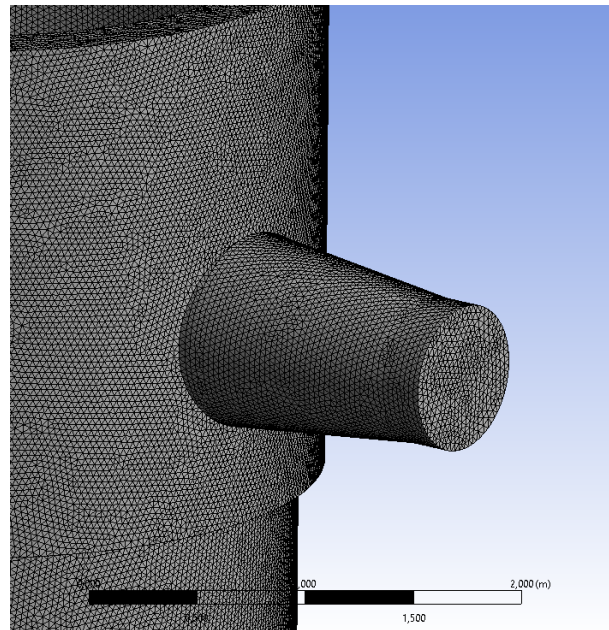


Figure 2. Meshing of cold leg and nearby RPV wall.

2.3 Initial and boundary conditions

The conditions were obtained from ref. [6]. The rationale for choosing the conditions was the following:

- observe the flow in the downcomer during normal operation;
- observe the flow in the downcomer at accident conditions, with the accident having already been previously considered (that is, simulated with a system code).

The fluid was set as water with a reference pressure of 155 bar and temperature 286 °C. Both inlet flows through cold legs were set to 4700 kg/s. The pressure drop in the vessel was estimated as 1.2 bar, so the outlet pressure was set to 153.9 bar.

3 RESULTS

3.1 Normal operation

As already stated, numerical simulations offer the opportunity to infer the flow pattern in the downcomer at operating conditions. In Figure 3, the magnitude of the axial velocity in the entire downcomer is presented. Some irregularities in the flow may be observed.

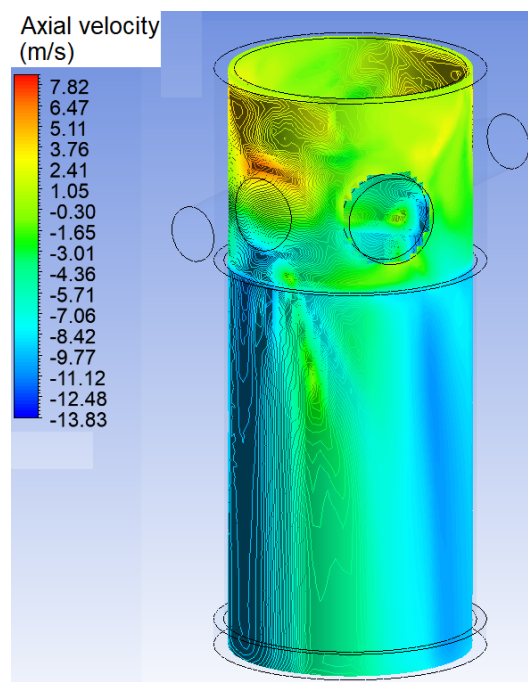


Figure 3. Normal operation: axial velocity contours.

The magnitudes of different velocities are shown at two different elevations (5 m from the bottom, which means a little below the cold legs, and at the bottom of the downcomer) in Figures 4-9. In almost all figures, almost perfect symmetry may be observed (but not complete symmetry, because of the cumulation of numerical errors), which is also an indication of the correctness of the numerical solving of the equations.

For the axial velocity (Figures 4 and 5), the velocities are in the same range at both elevations. However, the maximum axial velocity occurs at different circumferential locations, which is a consequence of the circumferential flow.

Incidentally, Figure 6 shows relatively high circumferential velocities at the upper level, which confirms the previous assertion about the influence of that flow. However, at the downcomer outlet (Figure 7), the values of the circumferential velocity are very low over the entire area, which indicates that the present design of the downcomer is adequate.

As expected, the radial velocity at the upper observed level (Figure 8) is the highest near the location of the cold legs. Basically, the impingement of the flow on the inner wall of the downcomer is a loss that cannot be avoided. However, the radial velocity at the downcomer outlet (Figure 9) is homogeneously low over the entire area, which confirms the adequacy of the design.

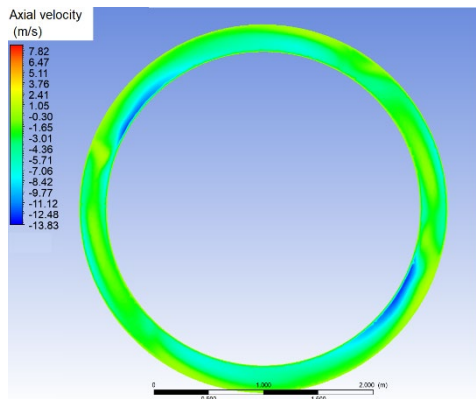


Figure 4. Normal operation: axial velocity 5 m from bottom.

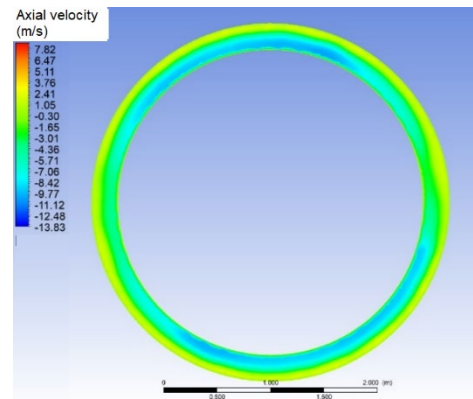


Figure 5. Normal operation: axial velocity at bottom.

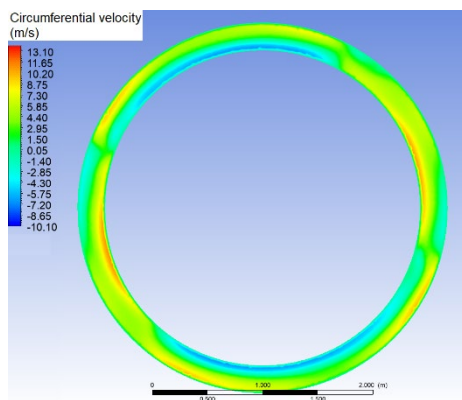


Figure 6. Normal operation: circumferential velocity 5 m from bottom.

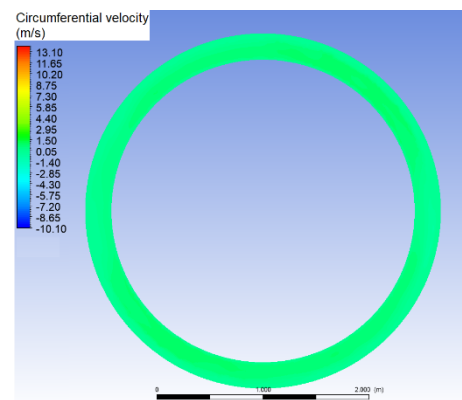


Figure 7. Normal operation: circumferential velocity at bottom.

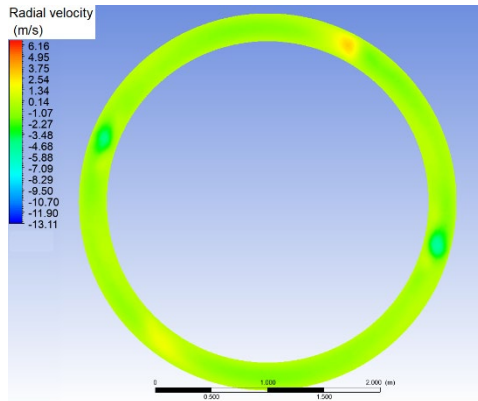


Figure 8. Normal operation: radial velocity 5 m from bottom.

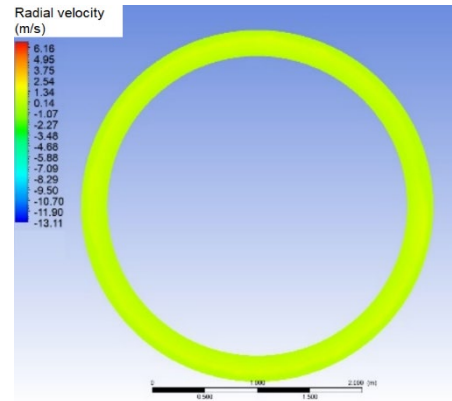


Figure 9. Normal operation: radial velocity at bottom.

3.2 Accident conditions

The simulation offers an opportunity to compare the flow in the downcomer at normal operation and at accident conditions. For the later, a small-break loss-of-coolant accident, simulated by Prošek et al. [6], was selected. After the actuation of the Emergency Core Cooling System, the mass flow rate in the broken cold leg is equal to 80 % of the value during normal operation. However, no apparent asymmetry is evident in the axial velocity at the level just below the cold legs (Figure 10). However, an asymmetry may be observed in the circumferential velocity, at the level just below the cold legs as well (Figure 11). Results at the downcomer outlet reveal that both the circumferential (Figure 12) and the radial velocity (Figure 13) are homogeneously low, which is beneficial for the cooling of the reactor core.

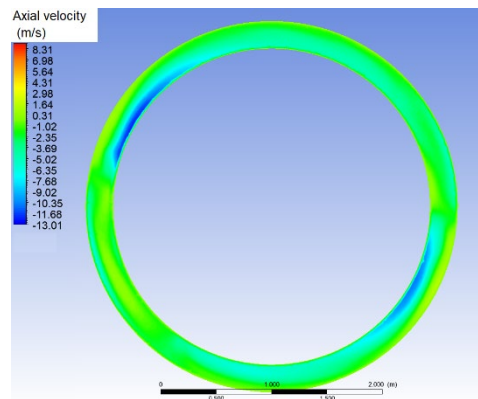


Figure 10. Break flow conditions: axial velocity 5 m from bottom.

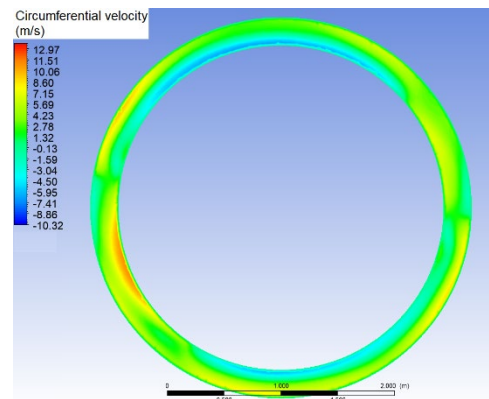


Figure 11. Break flow conditions: circumferential velocity 5 m from bottom.

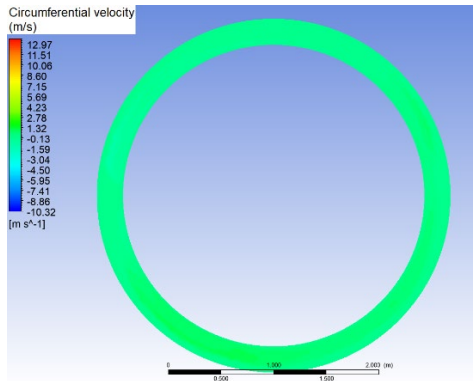


Figure 12. Break flow conditions: circumferential velocity at bottom.

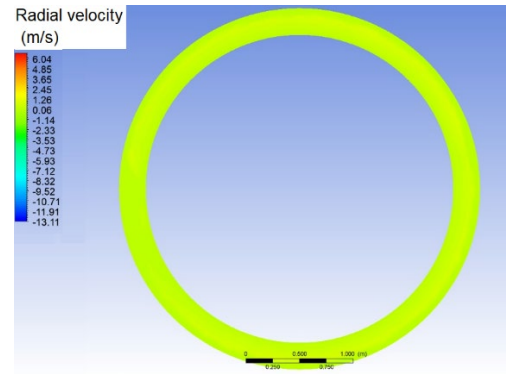


Figure 13. Break flow conditions: radial velocity at bottom.

3.3 Normal operation with obliquely mounted cold legs

The existing design of nuclear systems should by no means be considered as final, and possibilities for further development should still be investigated. However, the actual manufacturing of different systems is costly, which limits the possibilities of trying new designs. Simulations with CFD codes offer the possibility to visualise the behaviour of modified systems at much lower costs. Although the results cannot be considered as definitive proofs of the suitability of some new designs, they may still be used for the initial differentiation between different possibilities.

With this in mind, a model of a somewhat different design was developed, with both cold legs remaining in the same horizontal plane, but with an inclination of 30° instead of being mounted perpendicularly. The main rationale for this design was to decrease the impingement of the fluid injected through the cold legs on the downcomer inner wall.

A first impression of the flow may be seen in Figure 14, where streamlines are shown. The results should be compared with those for normal operation. The main differences may be observed at the upper observed level. That could have been expected, as the influence of the different orientation of the cold legs progressively vanes downwards. The comparison of axial velocities (Figures 15 and 16 vs. 4 and 5) shows larger regions with high velocity at the upper observed level, presumably as less kinetic energy is lost due to direct impingement on the downcomer inner wall. The comparison of circumferential velocities (Figures 17 and 18 vs. 6 and 7) shows somewhat higher velocities at the upper observed level as well, which was expected as the injected flow already has a circumferential component. Finally, the comparison of radial velocities (Figures 19 and 20 vs. 8 and 9) shows definitely much lower velocities at both observed levels, which was also expected.

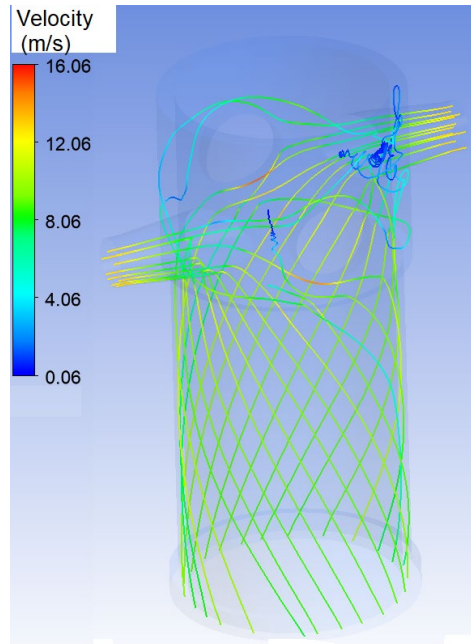


Figure 14. Streamlines with cold legs at 30° angle.

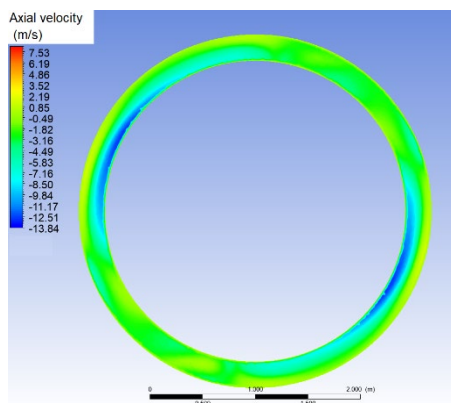


Figure 15. Cold legs at 30°: axial velocity 5 m from bottom.

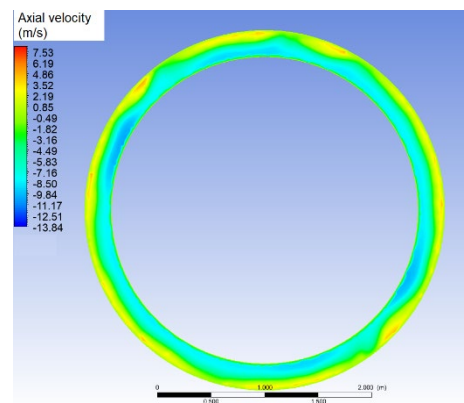


Figure 16. Cold legs at 30°: axial velocity at bottom.

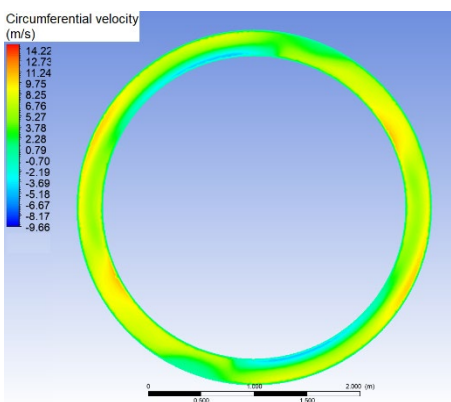


Figure 17. Cold legs at 30°: circumferential velocity 5 m from bottom.

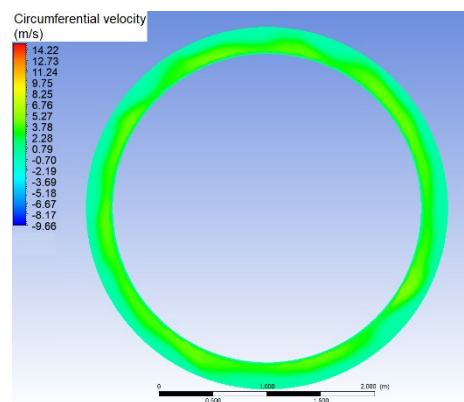


Figure 18. Cold legs at 30°: circumferential velocity at bottom.

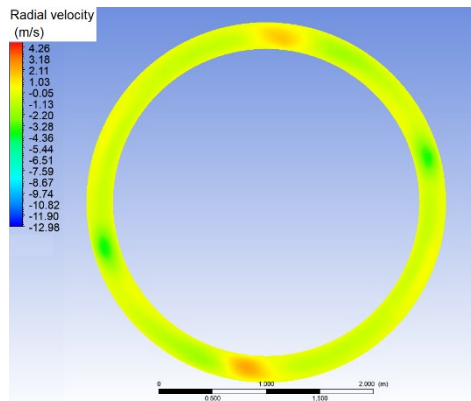


Figure 19. Cold legs at 30°: radial velocity 5 m from bottom.

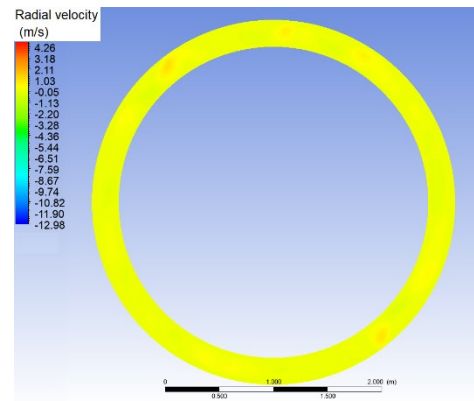


Figure 20. Cold legs at 30°: radial velocity at bottom.

4 CONCLUSIONS

The purpose of the presented work was to gain insights in the detailed flow pattern in the downcomer of the Reactor Pressure Vessel of a two-loop Pressurized Water Reactor, as it cannot be observed experimentally, as well as to observe the effects of a hypothetical modified design. The performed simulations reveal the flow pattern at normal operation, during a small-break loss-of-coolant-accident, and at normal operation with obliquely mounted cold legs. The results for normal operation show that at the downcomer outlet, the circumferential and radial velocity are homogeneously low. At accident conditions, the flow is asymmetric near the cold legs, but both non-axial velocities are homogeneously low at the downcomer outlet. The main influence of obliquely connected cold legs is the much lower radial velocity, which reflects mainly in larger regions with highest axial velocity. However, the differences are not such that significant effects on the mixing within the downcomer could be expected.

ACKNOWLEDGMENTS

The authors wish to thank Dr. Janez Kokalj from the Jožef Stefan Institute Reactor Engineering Division who provided the simplified model of the downcomer that was used as a basis for the development of the CFD model.

REFERENCES

- [1] G.M. Cartland Glover, T. Höhne, S. Kliem, U. Rohde, F.P. Weiss, H.M. Prasser, "Hydrodynamic Phenomena in the Downcomer During Flow Rate Transients in the Primary Circuit of a PWR," *Nuclear Engng Design*, 237, 732-748, 2006.
- [2] U. Rohde, T. Höhne, S. Kliem, B. Hemström, M. Scheuerer, T. Toppila, A. Aszodi, I. Boros, I. Farkas, P. Mühlbauer, L. Vyskocil, J. Klepac, J. Remis, T. Dury, "Fluid Mixing and Flow Distribution in a Primary Circuit of a Nuclear Reactor," *Nuclear Engng Design*, 237, 1639-1655, 2007.
- [3] M. Sharabi, V.F. Gonzalez-Albuixech, N. Lafferty, B. Niceno, M. Niffenegger, "Computational Fluid Dynamics Study of Pressurized Thermal Shock Phenomena in the Reactor Pressure Vessel," *Nuclear Engng Design*, 299, 136-145, 2016.

- [4] T. Höhne, S. Kleim, U. Bieder, "IAEA CRP Benchmark of ROCOM PTS Test Case for the Use of CFD in Reactor," *Nuclear Engng Design*, 333, 161-180, 2018.
- [5] S. Kliem, A. Grahn, Y. Bilodid, T. Höhne, "A Realistic Approach for the Assessment of the Consequences of Heterogeneous Boron Dilution Events in Pressurized Water Reactors," *Nuclear Engng Design*, 349, 150-161, 2019.
- [6] A. Prošek, I. Parzer, B. Mavko, "SB LOCA Analyses for Krško Full Scope Simulator Verification," *Proc. Int. Conf. Nuclear Energy in Central Europe 2000*, Bled, Slovenia, 2000.